

**Identifying Barriers and Least Cost Paths for
Autonomous Vehicle Navigation Using Airborne
LIDAR Data**

OM PRAKASH POUDEL

Thesis submitted to the faculty of
Virginia Polytechnic Institute and State University
in partial fulfillment of the requirements for the degree of

**MASTER OF SCIENCE
IN
GEOGRAPHY**

Laurence W. Carstensen, Ph.D., Committee Chair

James B. Campbell, Ph.D.

Charles F. Reinholtz, Ph. D.

Virginia Polytechnic Institute and State University

May 30, 2007

Blacksburg, Virginia 24061

Key words: LIDAR, Friction Surface, Accumulated Surface, Least-cost path

Identifying barriers and least cost paths for autonomous ground vehicle navigation using airborne LIDAR data

Om Prakash Poudel

Dr. Bill Carstensen (Advisor)

Abstract

In the past several years, the Defense Advanced Research Projects Agency (DARPA) has sponsored two Grand Challenges, races among autonomous ground vehicles in rural environments. These vehicles must follow a course delineated by Global Positioning System waypoints using no human guidance. Airborne LIDAR data and GIS can play a significant role in identifying barriers and least cost paths for such vehicles. Least cost paths minimize the sum of impedance across a surface. Impedance can be measured by steepness of slope, impenetrable barriers such as vegetation and buildings, fence lines and streams, or other factors deemed important to the vehicle's success at navigating the terrain. This research aims to provide accurate least cost paths for those vehicles using airborne LIDAR data. The concepts of barrier identification and least cost path generation are reviewed and forty-five least cost paths created with their performance compared to corresponding Euclidean paths. The least cost paths were found superior to the corresponding Euclidean paths in terms of impedance as they avoid barriers, follow roads and pass across relatively gentler slopes.

Attribution

Dr. Carstensen is my primary advisor for this research study and is Co-PI of the grant that funded this work. He helped in providing the outline of this research.

Dr. Campbell is a member of my thesis committee. He provided modifications and feedbacks on the methodology used.

Dr. Reinholtz is a member of my thesis committee and PI of the grant that funded this work. He helped to develop the detail methodology that suit autonomous vehicles.

ACKNOWLEDGEMENTS

During my studies at Department of Geography, Virginia Polytechnic Institute and State University, Blacksburg, VA and particularly during the preparation of this thesis, I have received both great personal assistance and profound technical education from many people.

I wish to express my heartfelt gratitude to my advisor Dr. Bill Carstensen for introducing me to the topic and constructive suggestions throughout the work. I am highly obliged to his kind help, support and supervision during the completion of this work.

My deep and cordial gratitude also goes to Dr. Jim Campbell for his candid input, instruction, and guidance through out my studies at Virginia Tech. I would also like to thank Dr. Charles Reinholtz for his input and support of this study.

I am very much indebted to all teachers and staffs of Department of Geography, Virginia Tech, for their inspirations and fruitful suggestions. Finally, I am thankful to my entire group of colleagues who provided me great decent assistance.

I would also like to thank Joint Unmanned Systems Testing Experimentation and Research (JOUSTER) for providing support to this study.

Last but certainly not the least, I express my deepest gratitude to my family members for their eternal help, support and inspiration.

Om Prakash Poudel

Table of Contents

	Page
Abstract	ii
Attribution	iii
Acknowledgements	iv
Table of Contents	v
List of Figures	vii
List of Tables	viii
Chapter 1: Introduction and Statement of Purpose.....	1
1.1 Introduction	1
1.1.1 LIDAR	1
1.1.2 Autonomous vehicle navigation	2
1.2 Statement of Purpose	2
Chapter 2: Literature Review	5
2.1 Introduction	5
2.2 Terms and Definitions	5
2.2.1 Digital Elevation Model and Digital Terrain Model	5
2.2.2 Normalized Digital Surface Model	5
2.2.3 Friction Surface	6
2.2.4 Accumulated Surface	6
2.3 Algorithms for LIDAR data segmentation	7
2.3.1 Morphological filters	7
2.3.2 Linear Prediction	8
2.3.3 Slope based	9
2.4 GIS algorithms for least cost paths	10
Chapter 3: Identifying barriers and least cost paths for autonomous vehicle navigation using airborne LIDAR data	16
3.1 Introduction	16
3.2 Related work	18
3.2.1 Identification of barriers	18
3.2.2 Morphology filtering.....	19
3.2.3 Weighting factors and constrains to create the friction surface	22
3.2.4 Generation of accumulated surface and designation of least cost path.....	25
3.3 The experiment.....	26
3.4 Conclusions	34

List of Figures

	Page
Figure 1.1: A LIDAR System	1
Figure 2.1: Digital elevation model (DEM) and Digital surface model (DSM).....	5
Figure 2.2: A normalized digital surface model (NDSM)	6
Figure 2.3: A sample friction surface in which higher values represent impedances to movement, and paths are attracted to the lower valued cells.....	6
Figure 2.4: An accumulated cost surface developed from a unit cost friction surface.....	7
Figure 2.5: Dijkstra and BFS search algorithms with barrier (adapted from Patel, 2004).....	11
Figure 3.1: A LIDAR System	17
Figure 3.2: Flow chart for identifying barriers using morphological filter.....	19
Figure 3.3: A Normalized Digital Surface Model (NDSM).....	19
Figure 3.4: Filters as used in raster models (adapted from ArcGIS 9.2).....	20
Figure 3.5: Derivation of Minimum height surface by running the filter multiple times.....	21
Figure 3.6: Buffer zone above the minimum height surface to incorporate local variation on the ground surface.....	22
Figure 3.7: Barriers identified after running the morphological filter.....	22
Figure 3.8: Friction surface generated using the model described in the text.....	23
Figure 3.9: Flow chart for the generation of friction surface.....	24
Figure 3.10: An accumulated cost grid and a Backlink grid.....	26
Figure 3.11 Digitized building margin overlaid on top of building extracted.....	27
Figure 3.12: Digital orthophoto of the study area.....	28
Figure 3.13: Least cost paths and the Euclidean paths.....	29

Figure 3.14: Distribution of the values of costs of least cost paths minus costs of Euclidean paths.....	30
Figure 3.15: Least cost paths and Euclidean paths joining points 5, 7 and 5,9.....	31
Figure 3.16: Comparison between the average slope of least cost paths and average slope of Euclidean paths.....	32
Figure 3.17: Comparison between the length of the least cost paths versus the length of the Euclidean paths.....	33

List of Tables

	Page
Table 3.1 Summary results of accuracy assessment.....	27
Table 3.2: Summary results of each category of paths in terms of average cost, average slope and average length (no. of cells).....	29
Table 3.3: Table showing the cost differential in different path types.....	30
Table 3.4: Results of t-test.....	32
Table 3.5: Mean sinuosity of the least cost paths.....	33

Chapter 1: Introduction and Statement of Purpose

1.1 INTRODUCTION

1.1.1 LIDAR

LIDAR is an active remote sensing technology that determines the distance to an object or surface using laser pulses. Like the similar radar technology, which uses radio waves instead of light, the range to an object is determined by measuring the time delay between transmission of a pulse and detection of the reflected signal. It provides a 3D (X, Y and Z) cloud of points which describe true ground and objects above the ground such as vegetated areas or human made features. These objects on the ground can be detected through filtering or Lidar point cloud processing techniques (Sithole and Vosselman, 2004).

Laser altimetry has been used for a variety of applications since the late 1960's including systems flown on the Apollo 15, 16 and 17 missions to the Moon to derive surface topography (Kaula *et al.*, 1974). Since then, airborne systems have been used to map regional topography around the world for a variety of geophysical purposes including volcanic hazard assessment, ice sheet elevation change, coastal erosion, and tree height derivation (*e.g.*, Garvin, 1996; Krabill *et al.*; 1995; Magnussen and Boudewyn, 1998). The main aim of a LIDAR survey is to provide accurate elevation information.

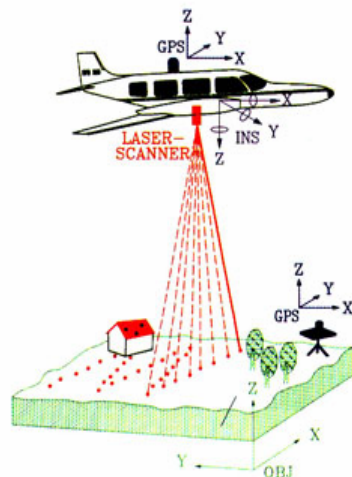


Figure 1.1: A LIDAR system (used with permission sbgmaps.com)

1.1.2 Autonomous vehicle navigation

Autonomous vehicles are robots which can travel from one place to another in unstructured environments without continuous human guidance. Although they do not require any human guidance after they start, they need source data and guidance systems (such as GIS, GPS and IMS) for the path along which they are meant to travel. GIS can provide an excellent database for providing the path to the autonomous vehicle if the terrain model provided is accurate.

1.2 STATEMENT OF PURPOSE

Human beings use their senses and brain to make complex decisions that enable them to function in complex environments. Machines lack both sense organs and brains and cannot do most human activities on their own, but scientists are trying to develop robots that resemble human beings and have the capacity of mimicking humans in some activities. Complete autonomy still remains to be seen. For example, for an autonomous vehicle to be truly intelligent it must access knowledge about its environment so it can navigate. How can vehicles be made to do this?

Humans have been using various tools for navigation for a long time. The technological progress has provided new tools to provide us with answers on how to get from point “a” to point “b”. Technology has greatly advanced navigation instruments making autonomous vehicle research possible. Vehicle sensors or machine vision can identify obstacles in a limited area, but cannot plan for what may lie a mile ahead. GIS is a solution to this problem as with a terrain database there is a way to navigate efficiently and develop long term routing. Lidar, being an efficient means to capture terrain data, should be paramount in use along with GIS to handle problems in navigation.

The first research objective is to use first return LIDAR data to identify objects that act as barriers to autonomous ground vehicles. After the barriers have been identified, different factors that affect the movement of vehicles are evaluated to determine optimal paths. Appropriate weight needs to be assigned to factors that affect vehicular movement and those factors summed

up to create a friction surface. The focus of this research is thus to develop a model that uses appropriate weights to create a friction surface. Once the friction surface is created it is used to generate accumulated surfaces and least cost paths between points in a study area. The evaluation of the least cost paths is then performed by comparing them to corresponding Euclidean paths.

Prior navigation research has not focused on LIDAR; hence this research aims at testing a potentially excellent database for autonomous vehicle navigation by using the terrain model provided by a LIDAR survey. Because a single pulse from the LIDAR unit can return from many surfaces other than the ground (Figure 1.1), LIDAR point clouds must be filtered before they can be used to generate a terrain model. So this research aims at providing an efficient model for: 1) identifying objects such as buildings and trees which serve as barriers to autonomous ground vehicles, and 2) for generating the optimal least cost path from the detailed terrain model derived from the LIDAR point cloud.

This research will generate several least cost paths and evaluate their performance in terms of cost, slope and length by comparing them with Euclidean paths. The Euclidean paths define the shortest physical distance benchmarks to quantify the cost, mean slope and sinuosity of the least cost paths. My hypothesis is that least cost paths are always better in terms of cost and slope than their corresponding Euclidean paths.

The results of this work will contribute to the navigation of autonomous ground vehicles by defining the model that gives trafficable areas and optimal paths using airborne LIDAR data.

Chapter 2 reviews research on object identification using airborne LIDAR data and application of GIS in navigation of autonomous vehicles. Chapter 3 focuses on generating a model that provides least cost paths for autonomous ground vehicle navigation and compares them to Euclidean paths.

References:

Kaula, W. M., Schubert, G., Longenfelder, R. E., Sjorgen, W. L., and Wollenhaupt, W. R. 1974, "Apollo laser altimetry and inferences as to lunar structure," *Geochim. cosmochim. Acta*, **38**, 3049-3058

Garvin, J. B. 1996, "Volcano Instability on the Earth and Planets" *Geological Society of London Special Public. 110*

Bamber, J. L., Ekholm, S. and Krabill, W. B. 2001, "A new, high-resolution digital elevation model of Greenland fully validated with airborne laser altimeter data," *J. Geophys. Res.*, *106*(D4), 6733–6745

Magnussen, S. and Boudewyn, P. 1998, "Derivations of stand heights from airborne laser scanner data with canopy-based quantile estimators" *Can. J. For. Res.*, **28**, 1016-1031,

Sithole, G. and Vosselman, G. 2004, "Experimental comparison of filter algorithms for bare-Earth extraction from airborne laser scanning point clouds," *ISPRS Journal of Photogrammetry and Remote Sensing*. *59*, pp. 85- 101

Chapter 2: Literature Review

2.1 INTRODUCTION

This chapter provides background on current algorithms and models for identifying objects from LIDAR point clouds and generation of least cost paths. I start with definitions of the terms that are widely used throughout this thesis (Section 2.2). I provide basic concepts and brief overview of the algorithms developed to separate objects from the ground surface in section 2.2. In section 2.3 I discuss GIS models and algorithms developed for least cost path generation.

2.2 TERMS AND DEFINITIONS:

2.2.1 Digital Elevation Model (DEM) and Digital Surface Model (DSM)

A bare ground surface without any objects is known as a minimum height surface (MHS) or a digital elevation model (DEM). A ground surface along with all the objects on it is known as Digital Surface Model (DSM) (Figure 2.1). First return airborne LIDAR data provide a DSM from which the objects are extracted to form a DEM.

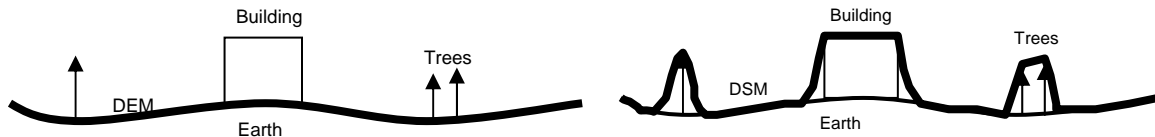


Figure 2.1: Digital elevation model (DEM) and Digital surface model (DSM)

2.2.2 Normalized Digital Surface model (NDSM)

The difference between the DSM and the DEM is known as normalized digital surface model (NDSM). In NDSM the objects appear to sit upon a level plain (Figure 2.2). Both the DEM and NDSM are derived from DSM so the first data to be processed for object identification is the DSM.



Figure 2.2: A normalized digital surface model (NDSM)

2.2.3 Friction Surface

A friction surface is comprised of cells whose values represent the cost of movement through them (Figure 2.3). The accumulated surface is created out of a friction surface hence the friction surface is the most significant factor in developing more realistic accumulated surfaces. Different factors and constraints layers are appropriately weighted and summed together to create a friction surface.

5	4	3	3	4	1	1	1
5	5	3	4	1	4	2	2
4	4	5	2	3	4	2	3
5	4	2	2	3	2	3	3

Figure 2.3: A sample friction surface in which higher values represent impedances to movement, and paths are attracted to the lower valued cells.

2.2.4 Accumulated Surface

An accumulated surface is represented by the Z coordinate value, the cost of movement to (from) any point X_i, Y_i from (to) a point of reference X_o, Y_o (clearly, $Z_o = 0$) (Warntz, 1961). Accumulated surfaces help us to calculate the least cost path between a source and a target. Costs of cells in the accumulated surface represent cumulative cost from a source location. On a homogeneous plane the accumulated cost surface is an inverted cone, centered on the point of reference and fully described by a mathematical model (Figure 2.4). As geographic surfaces are

very rarely homogenous or isotropic, GIS based accumulated surfaces are far more complex, but can be developed by an accumulation algorithm.

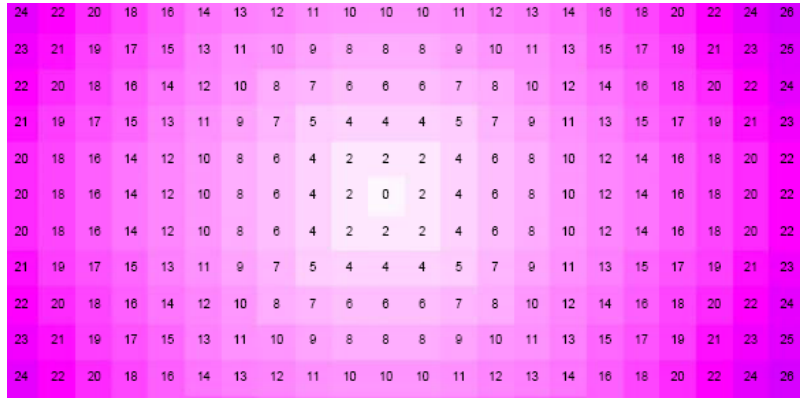


Figure 2.4: An accumulated cost surface developed from a unit cost friction surface

2.3 ALGORITHMS FOR LIDAR DATA SEGMENTATION

Over the past years, several filtering algorithms have been designed to extract bare-earth and objects from LIDAR point clouds. The most fundamental types of filters are outlined below.

2.3.1 Morphological filters:

An effective algorithm for removing non-ground objects is a morphology filter applied to grid format images. Kilian et al. (1996) proposed a method to remove non ground points using a morphological filter. Morphology filters assume that a ground point's height is lower than its neighboring objects points and that there is no abrupt change on the ground, that is, that the ground surface is relatively smooth over short distances. Weidner and Forstner (1995) and Morgan and Habib (2000) have studied the separation of ground surface and objects from airborne LIDAR data using a morphology filter with good results.

The selection of a filtering window size and the distribution of the buildings and trees in a specific area are critical for the success of this method. If a small window size (3x3 cells for instance) is used in Kilian's method, most of the ground points will be preserved. However, only

small non-ground objects such as cars and trees will be effectively removed. On the other hand, the filter tends to remove too many ground points with a large window size (21 x 21 for instance). For example, road surface points next to drainage canals will be removed completely if the window size is larger than the width of a road. In addition, the tops of local mounds and sand dunes in flat coastal areas are often “chopped off” by using a large size window. Ideally, the window size of the morphological operation should be small enough to preserve all ground details and large enough to remove buildings, cars, and trees. Unfortunately, a single ideal window size does not exist in the real world. To avoid this conflict, Kilian et. al. (1996) proposed multiple applications of different window sizes, starting from the smallest size.

There are other modifications available for this type of filter as well. Lohmann et al. (2000) used a dual-rank morphological filter proposed by Eckstein and Munkelt (1995) to classify LIDAR point data. Zhang et al. (2003) used a progressive morphological filter to remove non-ground measurements from airborne LIDAR data.

2.3.2 Linear Prediction:

The linear prediction method (Kraus and Pfeifer, 1998) is based on calculation of the distance from an average surface to the measurement points. The classification of original points is based on a hierarchical method. At each hierarchy level, robust interpolation for the classification of the points and surface derivation is done. A rough approximation of the terrain is first computed using the points of the respective hierarchy level. The vertical distance of the points to this approximate surface is then used in a function to assign weights to all points. Points above the surface are given a small weight and those below the surface are given large weight. The surface is then recomputed using a linear interpolation (similar to kriging) considering individual weights. In this way the recomputed surface is attracted to the low points. The process is iterated until a specified number of iterations have been reached or the computed surface does not change significantly between iterations.

2.3.3 Slope based:

Algorithms developed by Vosselman (2000), Vosselman and Maas (2001), Sithole (2001) and Roggero (2001) fall in this category. In these algorithms, the slope or height difference is measured. If the slope exceeds a certain threshold, then the highest point is assumed to belong to an object.

In Vosselman's filter (Vosselman, 2000; Vosselman and Maas, 2001), a local operator is centered at each point and applied to a point's neighborhood. The operator is generally an inverted funnel (or a cone). If there are no points beneath the inverted funnel, then the point at the center of the inverted funnel is accepted as bare-earth. The remaining points are objects. The inverted funnel applied at each point is the same.

Both the Sithole and Roggero's filter are variants of the Vosselman's filter tailored to obtain better performance. In Roggero's filter, the shape of the inverted funnel is adapted to the slope of the bare earth at a point. Because the bare-earth is not known, it is estimated using a local linear regression criterion.

The filter developed by Sithole resembles Roggero's, but to improve the performance of the algorithm in steep terrain, the slope of the cone matched to slope of the terrain. The slope of the terrain is computed from a rasterized slope map, from the lowest points in each cell.

As all of these filters make basic assumptions about their neighborhoods, the effectiveness of their performance varies from landscape to landscape. As such all of these filters are application dependent and their performance varies from landscape to landscape. Sithole and Vosselman (2004) made an experimental comparison of most of the available filters. They conclude that all filters work quite well in landscapes of low complexity (characterized by gently sloped terrain, small buildings, sparse vegetation, and a high proportion of bare-earth points). But, complex cityscapes and discontinuities at the bare earth cause the greatest problems.

2.4 GIS ALGORITHMS FOR LEAST COST PATHS

Computation of the least cost path is not a new concept within geographic information systems. There have been several useful applications of least cost paths reported in the recent past such as selecting the best route for a pipeline based on land use and land cover data (Feldman et al., 1996) and selecting the cheapest route to transport commodities based on land use and topographic data (Jaga et al., 1993).

There are two types of mapping systems in autonomous ground vehicles. The local map is built from data gathered by the onboard sensors. The least cost paths generated from the GIS are commonly referred to as the global map. Vandapel et al. (2006) state that an autonomous ground vehicle using on-board sensors only is very unlikely to select an optimal path to traverse a given terrain, facing dead-ends or missing less dangerous areas, out of reach of its sensors. Hence the use of a priori data helps to cope with such problems by providing information to perform global path planning.

Although GIS have been used in path planning for several other cases, only a few studies have examined global path planning for autonomous ground vehicles (Stahl, 2005, Frederick et al., 2005 and Vandapel et al., 2006).

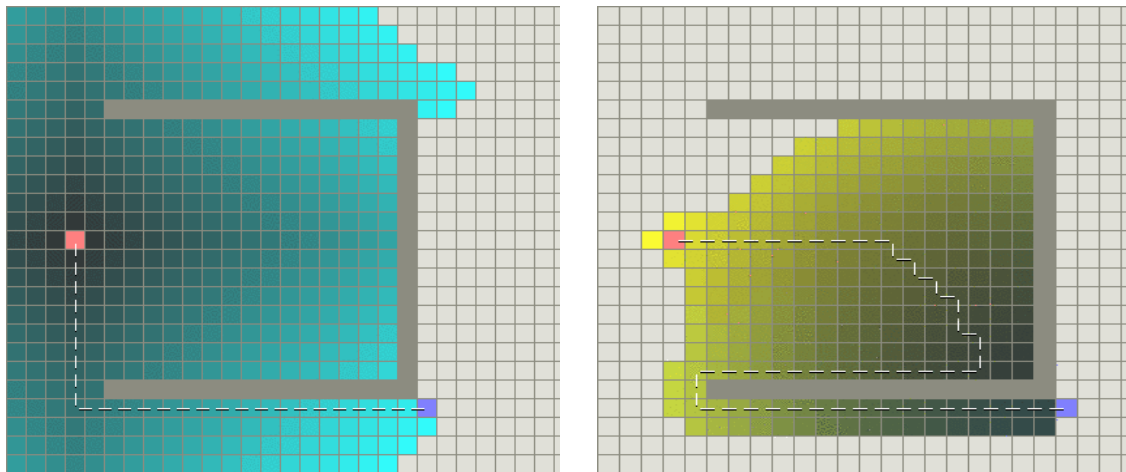
A realistic friction surface is required for planning optimal paths. Stahl (2005) has done sensitivity analysis to see how different factors need to be weighted to generate a realistic friction surface. Frederick et al. (2005) have looked at different attributes that are important for navigation of autonomous vehicles and assigned them as 'go' or 'no go' according to their behavior. Vandapel et al. (2006) used airborne LIDAR data to compute traversability maps for autonomous ground vehicles in highly vegetated areas.

Of the few basic algorithms that have been used for routing applications, the most popular is Dijkstra algorithm (Patel, 2004). The cost accumulation process in this algorithm starts from the target (starting point), grows outward in an expanding cell neighborhood ending up at the source (ending point), accumulating cost values for all the cells. From the starting point each cell is

examined in order of distance and the algorithm iteratively searches for the next closest cell in terms of cost from the friction surface. For every cell traveled from the starting point cost increases until the ending point is found.

The Best First Search (BFS) (Patel, 2004) searches for a path quickly by accumulating a small number of cells in a heuristic manner. BFS estimates the distance from the start point to the end point. Because of this estimate, it selects cells closer to the end point for accumulation before it selects the cells near the start point. Because fewer cells are accumulated in this method, it does not guarantee optimal solution like the Dijkstra algorithm (Figure 2.5).

The A* (Patel, 2004) algorithm combines the reliability of Dijkstra algorithm and performance of the BFS algorithm and guarantees the shortest path. It is considered an admissible heuristic algorithm because it never over-estimates the distance or cost from a cell to the end point. Most available GIS software does not use A* but accumulates the whole surface.



A. Dijkstra with barrier (Dark cyan cells represents less cost than those that are brighter) **B.** BFS with barrier (Dark yellow cells represents less cost than those that are brighter)

Figure 2.5: Dijkstra and BFS search algorithms with barrier (Pink cell the starting point and purple cell is the end point) (used with permission, Patel, 2004)

GIS uses a cost surface function based on the node/link cell representation used in graph theory to determine the cost for a path to pass through cells to reach a source. In the node/link cell representation, each cell center is considered a node and each node is connected by multiple links. The impedance of the link is derived from the costs associated with the cells at each end of the link (obtained from the friction surface) and the direction of movement through the cells.

The cost allocation function identifies, for each cell, which source would be the least costly to reach using a spread function (Lee and Stucky, 1998). A spread function starts with the node of the source cell. In the first iteration, the cumulative cost of each of the neighboring eight cells is computed and recorded in the corresponding cells of the accumulated surface grid. Then it moves to the cell which has the lowest value and the search begins in the similar way to the previous iteration. This search continues until all the cells of the friction surface have a corresponding value of accumulated cost in the accumulated surface grid.

The least cost path procedure creates a cumulative cost grid and a backlink grid from the friction surface used. For each cell in the friction surface, the cumulative cost grid stores the total travel cost to the destination point. The backlink grid indicates the direction of the least cost path from any cell to the destination point using a number of systems to represent directions. Whenever a beginning point is designated, the backlink grid indicates the direction that the path should follow; from the beginning point all the way to the destination point. A least cost path consists of sequentially connected links that provide the route for each cell location to reach a source cell. The least-cost path distance from a cell to a source cell is the minimum cost distance among all cost path distances from the cell to the source cells (ArcGIS 9.2, 2007).

References:

ArcGIS 9.2 desktop help, 2007, Environmental Systems Research Institute (ESRI)

Edwards, D. L., Desmond, G. B. and Schoppmann, M.W. 1988, "Terrain Database Generation for Autonomous Land Vehicle Navigation," *Photogrammetria* 43: 101-107.

Feldman, S. C., Pelletier, R. E., Walser, E., Smoot, J. C. and Ahl, D. 1996, "GIS, remote sensing analysis used to select potential route," *Pipe Line and Gas Industry*, May 1996, 52 – 55.

Jaga, R., Novaline, M., Sundaram, A., and Natarajan, T. 1993, "Wasteland development using geographic information system techniques," *International Journal of Remote Sensing*, 14, 3249 – 3257.

Kilian, J., Haala, N., and English, M. 1996, "Capture and evaluation of airborne laser scanner data," *Int. Arch. Photogramm. Remote Sens.*, vol. 31, pp. 383–388.

Kraus, K., and Pfeifer, N. 1998, "Determination of terrain models in wooded areas with airborne laser scanner data," *ISPRS Journal of Photogrammetry and Remote Sensing* 53 (5), pp. 245-261

Lee, J. and Stucky, D. 1998, "On applying viewshed analysis for determining least-cost paths on Digital Elevation Models," *International Journal of Geographical Information Science*, Vol. 12, No. 8, 891- 905

Lohmann, P., Koch, A. and Schaeffer, A. 2000, "Approaches to the filtering of laser scanner data," *International Archive on Photogrammetry and Remote Sensing*, pt. B3, vol. 33, pp. 540–547.

Morgan, K and Habib, A., 2002, "Interpolation of LIDAR data and automatic building extraction," Proceeding of ACSM – ASPRS 2002 Annual Conference, Washington D.C. (CD – ROM)

Patel, A. J. 2004. Amit's Game Programming Site. "Amit's Thoughts on Path-Finding and A-Star." <http://theory.stanford.edu/~amitp/GameProgramming/> (Last Accessed 11 May 2007).

Sithole, G., 2001, "Filtering of laser altimetry data using a slope adaptive filter," IAPRS, 34, 3W4

Sithole, G. and Vosselman, G., 2004, "Experimental comparison of filter algorithms for bare-Earth extraction from airborne laser scanning point clouds," ISPRS Journal of Photogrammetry and Remote Sensing 59, 85-101

Stahl, C. 2005, "Accumulated Surfaces & Least-Cost Paths: GIS Modeling for Autonomous Ground Vehicle (AGV) Navigation," Thesis submitted to the Department of Geography, Virginia Tech

Vandapel, N., Donamukkala, R., Hebert, M. 2006, "Unmanned ground vehicle navigation using aerial Ladar data," The international journal of robotics research, Vol. 25, No. 1, pp. 31- 51

Vosselman, G. 2000, "Slope based filtering of laser altimetry data," International archives of the photogrammetry, remote sensing and spatial information sciences XXXIII (Pt. B3) 935 – 942.

Vosselman, G., Maas, H., 2001, "Adjustment and filtering of raw laser altimetry data," Proc. OEEPE workshop on Airborne Laserscanning and Interferometric SAR for detailed digital elevation models, 1-3 March, OEEPE Publication no. 40, 11pp. (on CD-ROM)

Warntz, W. 1961, "Transatlantic flights and pressure patterns", The Geographical Review, Vol. 51, 187-212, 1961

Weidner, U and Forstner, W. 1995, "Towards automatic building extraction from high resolution digital elevation models," ISPRS Journal of Photogrammetry and Remote Sensing, Vol.50 pp 38 – 49

Zhang, K., Chen, S., Whitman, D., Shyu,M., Yan, J. and Zhang, C. 2003, "A progressive morphological filter for removing nonground measurements from airborne LIDAR data," IEEE Transactions on geoscience and remote sensing, Vol. 41, No. 4 pp 872-882

Chapter 3: Identifying barriers and least cost paths for autonomous ground vehicle navigation using airborne LIDAR data *

*This chapter is a manuscript in preparation for submission to GIScience and Remote Sensing journal

Om Poudel, Bill Carstensen

*Department of Geography, Virginia Polytechnic Institute and State University,
Blacksburg, VA 24061*

Abstract: In the past several years, the Defense Advanced Research Projects Agency (DARPA) has sponsored two Grand Challenges, races among autonomous ground vehicles in rural environments. These vehicles must follow a course delineated by Global Positioning System Waypoints using no human guidance. Airborne LIDAR data and GIS can play a significant role in identifying barriers and least cost paths for such vehicles. Least cost paths minimize the sum of impedance across a surface. Impedance can be measured by steepness of slope, impenetrable barriers such as vegetation and buildings, fence lines and streams, or other factors deemed important to the vehicle's success at navigating the terrain. This research aims at providing accurate least cost paths for those vehicles using airborne LIDAR data. The concepts of barrier identification and least cost path generation are reviewed and forty-five least cost paths created with their performance compared to corresponding Euclidean paths. The least cost paths were found superior to the corresponding Euclidean paths in terms of impedance as they avoid barriers, follow roads and pass across relatively gentler slopes.

Key words: LIDAR, Friction Surface, Accumulated Surface, Least-cost path

3.1 INTRODUCTION

LIDAR is an active remote sensing technology that uses pulses of light to determine the distance to an object or surface using laser pulses. Like radar technology, which uses radio waves instead of light, the range to an object is determined by measuring the time delay between transmission of a pulse and detection of the reflected signal (Figure 3.1). It provides a 3D (X, Y and Z) cloud of points which describe both the true ground surface and objects belonging either

to vegetated areas or to human made features. These objects above the ground can be detected through filtering or Lidar point cloud processing techniques (Sithole and Vosselman, 2004).

ESRI defines a least cost path as, “The path between two locations that costs the least to traverse, where cost is a function of time, distance, or some other criteria defined by the user” (ArcGIS desktop help 9.2, 2007). The computation of a least cost path is a useful application of geographic information systems (GIS) that have been in use for decades now. Use of high resolution LIDAR data in identifying barriers and least cost paths for autonomous vehicle navigation in an unstructured terrain has just begun to be researched and has only now gained some acceptance. Since it is extremely precise, airborne LIDAR data can be used in barrier identification and path planning for such vehicles to provide more accurate results than previous attempts using standard Digital Elevation data. In addition, because it captures the entire land surface including objects built or growing on it, LIDAR data can provide more complete information to routing algorithms.

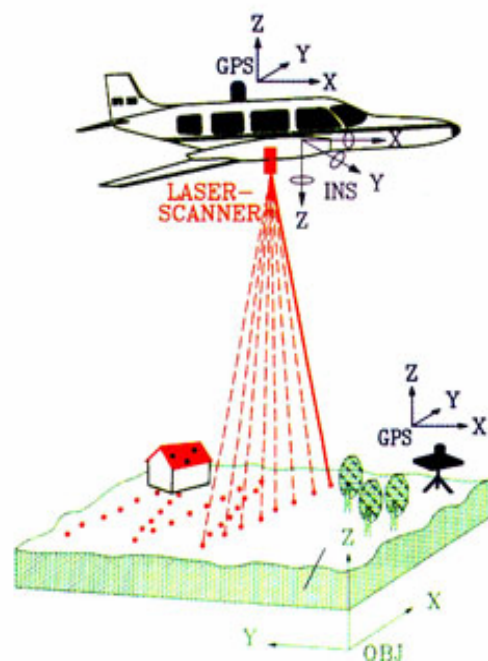


Figure 3.1: A LIDAR System (used with permission, sbgmaps.com)

The ultimate objective of identifying least cost paths for autonomous ground vehicles is to provide an optimal path for navigation. The data used can be LIDAR data, imagery data or other GIS layers. But, since LIDAR data has high vertical accuracy, its use along with these other data sets can be extremely helpful. This research develops and tests a model to identify barriers and to generate least cost paths for autonomous ground vehicles in an unstructured terrain using airborne LIDAR data.

3.2 RELATED WORK

3.2.1 Identification of barriers:

For autonomous vehicles, barriers appropriate to detection by LIDAR are objects too large to drive over, or slopes too steep to traverse. Vehicle barriers are objects in a point cloud that stand above the ground surface, such as vegetation (trees or shrubs) or buildings. Extreme slopes also form barriers as part of the ground surface. Other barriers such as rivers and fences can be derived from other GIS data layers more effectively than from LIDAR data.

The flowchart in Figure 3.2 gives the general overview of the process involved in identifying barriers. Raw LIDAR (first return points) data are not well suited to perform barrier identification. More amenable is one of two intermediate products: a triangulated irregular network (TIN) or raster format image (grid). Both TINs and grid images can be created from raw LIDAR data, but in our experience it is more efficient to create a TIN and then to convert it to a grid. This grid which contains all the information about the terrain including the buildings and trees is known as a digital surface model (DSM) in the GIS and remote sensing community. Along with the DSM, other useful products for a GIS are the Minimum Height Surface (MHS) more commonly known as a Digital Elevation Model (DEM) and the objects on the MHS. The process of separating the MHS from DSM is known as LIDAR data segmentation.

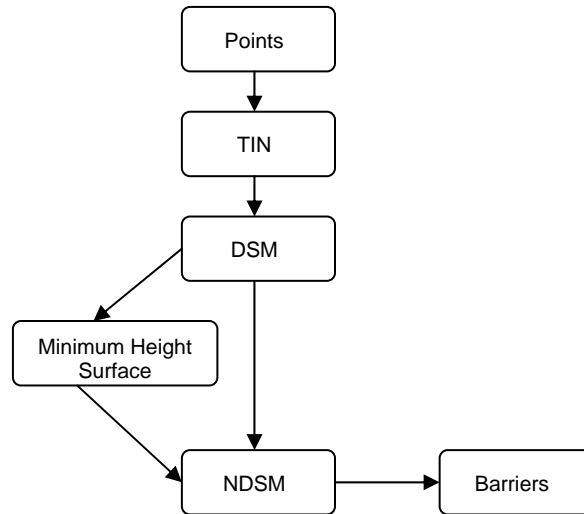


Figure 3.2: Flow chart for identifying barriers using morphological filter

In order to identify objects, the DSM is generated first, and then a MHS and finally a normalized DSM (NDSM). A NDSM is a surface relative to the MHS. Objects within a NDSM are viewed as sitting on a level plane (Figure 3.3). Based on the assumption that a ground point's height is lower than its neighboring object points and that the ground is fairly smooth, morphology filters are most effective to distinguish ground points in a LIDAR data set.



Figure 3.3: A Normalized Digital Surface Model (NDSM)

3.2.2 Morphology filtering:

One of the most widely used post-processing algorithms uses morphology filters to separate the ground from the objects. Morphology filters assume that a ground point's height is lower than its neighboring objects points and that there is no abrupt change on the ground, that is that the ground surface is relatively smooth over short distances. Weidner and Forstner (1995) and

Morgan and Habib (2000) have studied the separation of ground surface and objects from airborne LIDAR data using a morphology filter with good results.

The procedure of morphology filtering can be summarized as following.

- a. Create the MHS: Based on a prior knowledge of the largest object (such as a building) to be identified within the study area, set the window size of a morphology operator to be just larger than the largest building. This window defines the neighbors of a pixel for the analysis. For each pixel of a DSM grid, the pixels within the neighborhood are checked and their height values are compared. The minimum value in its neighborhood is assigned to the central cell. In GIS software, a minimum filter serves this purpose by looking in a neighborhood and reporting the smallest elevation value in that region (Figure 3.4). Filters in raster models are typically 3 x 3 with the result stored in the central cell, however, as noted above, the optimal size of the filter in this application depends upon the size of the objects expected to be found in study area. In some cases, if the largest buildings are very large, with a particular filter size, all the surface objects might not be removed by running the filter only once. Rather, the filter must be run two or more times until none of the above ground objects remain in the filtered dataset (Figure 3.5). The need to continue to run the filter can be assessed visually by comparing the minimum height surface with the original surface. After the minimum height surface is generated, it is overlaid with the original surface and the objects are identified by looking for rapid variations in heights among neighboring points.

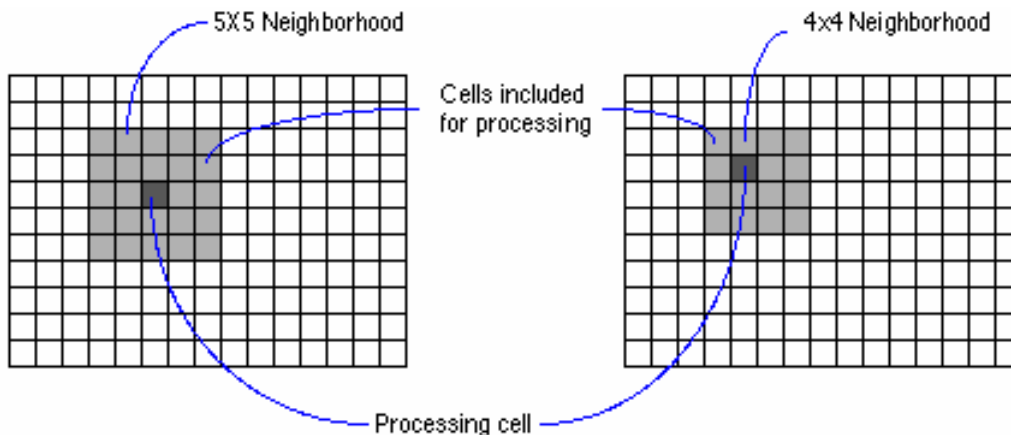


Figure 3.4: Filters as used in raster models (used with permission © esri.com)

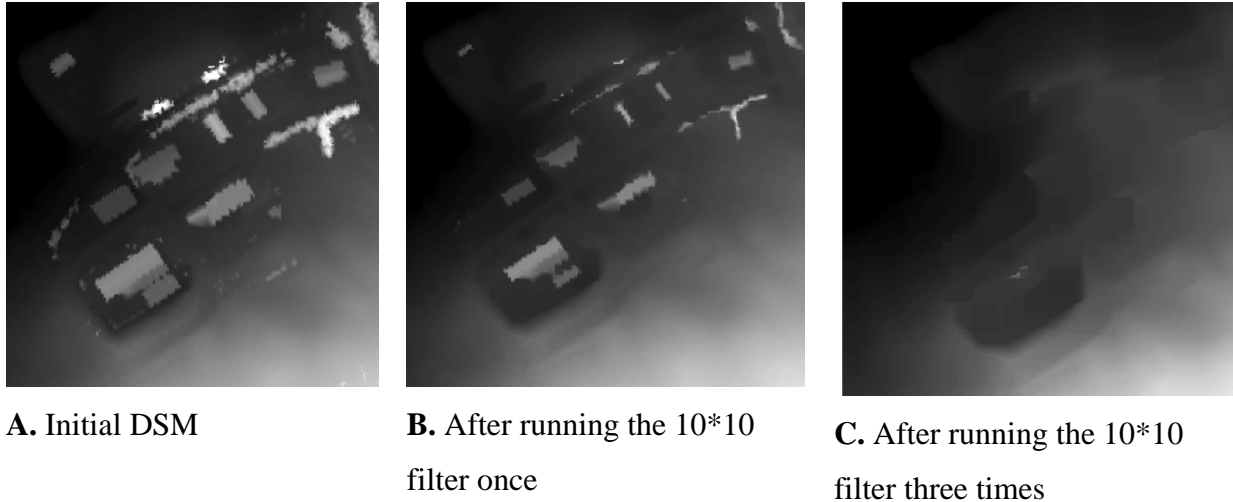


Figure 3.5: Derivation of Minimum height surface by running the filter multiple times

- b. Remove Barriers: The selection of a filtering window size and the distribution of the buildings and trees in a specific area are critical for the success of morphological filtering (Zhang et al. 2003). If a small window size is used, most of the ground points will be preserved but only small non-ground objects such as cars and trees will be effectively removed. On the other hand, the filter tends to remove too many ground points with a large window size. For example, the tops of local mounds and sand dunes in flat coastal areas can be “chopped off” by using a large window size. Ideally, the window size of the morphological operation should be small enough to preserve all ground details and large enough to remove buildings, cars, and trees. Unfortunately, an ideal window size does not exist in the real world. Thus, if the filtering window size is large because of the large objects present on the study area, it removes local variations in the ground surface (like small ditches and ramps). Hence to allow such variations, a filter of the size of the largest building to be removed is run and then a buffer of some feet is taken above the minimum height surface (Figure 3.6).

All the points inside that buffer zone are regarded as ground surface and those above as objects. The buffer distance selected depends largely on the resolution of the data, type of surface, capacity of the vehicle to climb over steep objects which could be left behind and the size of filter used. A sensitivity analysis with different buffer heights was used to

determine the effect of this parameter on surface object identification until the optimal value (5 feet in this case) was found. Figure 3.7 shows the barriers identified using this method in our test area.

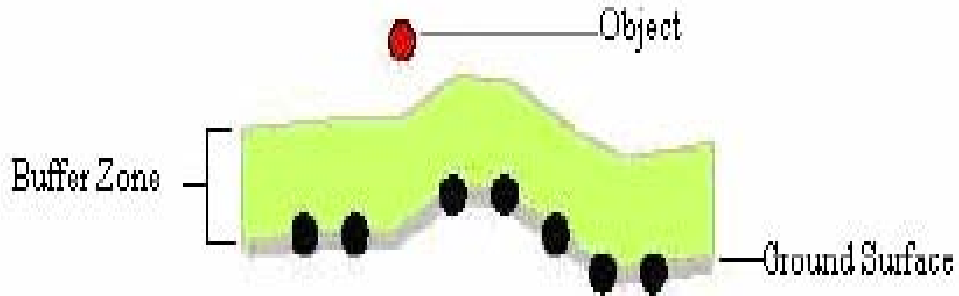


Figure 3.6: Buffer zone above the minimum height surface to incorporate local variation on the ground surface

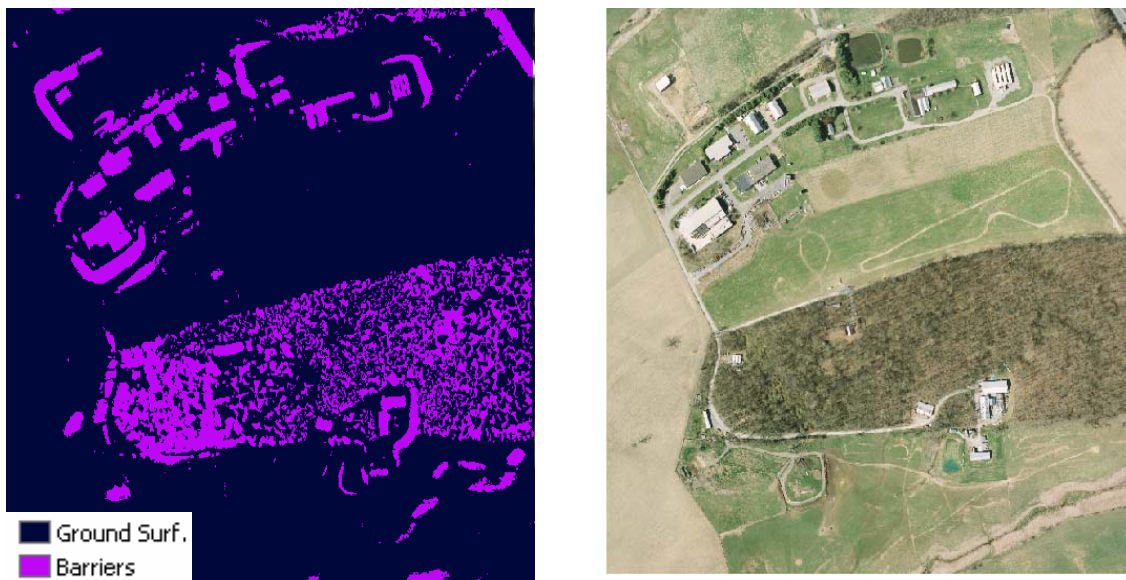


Figure 3.7: Barriers identified after running the morphological filter (Image used with permission © blacksburg.gov)

3.2.3 Weighting factors and constraints to create the friction (cost) surface

A friction surface is comprised of cells whose values represent the cost of movement across them (Figure 3.8). Several factors should be weighted and summed to generate a realistic friction surface. Depending upon the designated importance of each criterion, the friction surface is

weighted accordingly in the calculation of the least-cost paths. Data that the military collects for mobility modeling include slope, land cover, hydrography, and roads (Edwards, 1988). These are the factors that most influence navigation.

Computation of the least cost path is not a new concept within geographic information systems. There have been several useful applications reported using this function. Two especially pertinent to this research are selecting the best route for a pipeline based on land use and land cover data (Feldman et al., 1996) and selecting the cheapest route to transport commodities based on land use and topographic data (Jaga et al., 1993).



Figure 3.8: Friction surface generated using the model described in the text

Research on use of least cost path for autonomous vehicle navigation has also been done by Stahl (2005). He has done sensitivity analysis in his research to see how different factors need to be weighted to generate a realistic friction surface that would avoid steeper slopes than a vehicle could traverse and follow roads whenever practical. This research aims at making some improvement over that of Stahl by incorporating a LIDAR dataset in such analysis.

The flow chart in Figure 3.9 summarizes the processes involved in weighting factors and creating a friction surface. All obstacle layers are fused together into one layer that represents absolute barriers for traveling across the study area. The barriers designated in the step above are added to other constraining features, such as slopes over 15% or water bodies large enough to act as absolute barriers to vehicles. For all of these, cost is assigned as relatively higher than elsewhere, in this case a value of 500. Trafficable slopes are relative barriers and they are assigned incremental costs. Roads act as a catalyst for travel and have the lowest cost possible to encourage movement along them whenever practical to the direction of the target from the origin.

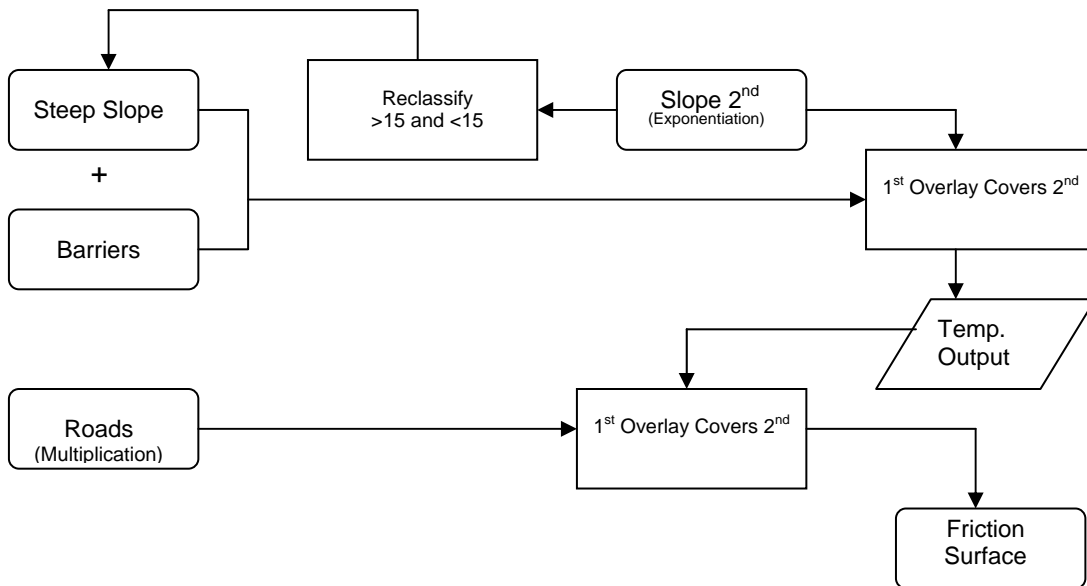


Figure 3.9: Flow chart for the generation of friction surface

To address the issue of how trafficable slopes and roads should be weighted; a sensitivity analysis was performed by Stahl (2005) to choose the most appropriate cost weights. This research uses his findings with some modification to determine the cost of trafficable slopes and roads. Slope percentage has been exponentiated by 1.1 and the cost of the road has been set as 0.8.

3.2.4 Generation of an accumulated surface and designation of the least cost path

An accumulated surface is represented by the Z coordinate value, the cost of movement to (from) any point X_i, Y_i from (to) a point of reference X_o, Y_o (clearly, $Z_o = 0$) (Warntz, 1961). On a homogeneous plane the accumulated cost surface is an inverted cone, centered on the point of reference and fully described by a mathematical model. As geographic surfaces are very rarely homogenous or isotropic, GIS based accumulated surfaces are far more complex, but can be developed by an accumulation algorithm.

GIS uses a cost surface function based on the node/link cell representation used in graph theory to determine the cost for a path to pass through cells to reach a source. In the node/link cell representation, each cell center is considered a node and each node is connected by multiple links. The impedance of the link is derived from the costs associated with the cells at each end of the link (obtained from the friction surface) and the direction of movement through the cells.

The cost allocation function identifies, for each cell, which source would be the least costly to reach using a spread function (Lee and Stucky, 1998). A spread function starts with the node of the target cell. In the first iteration, the cumulative cost of each of the neighboring eight cells is computed and recorded in the corresponding cells of the accumulated surface grid. Then it moves to the cell which has the lowest value and the search begins in the similar way to the previous iteration. This search continues until all the cells of the friction surface have a corresponding value of accumulated cost in the accumulated surface grid (Figure 3.10 A).

The least cost path procedure creates a cumulative cost grid and a backlink grid (Figure 3.10 B) from the friction surface. For each cell in the friction surface, the cumulative cost grid stores the total travel cost to the target. The backlink grid indicates the direction of the least cost path from any cell to the target using a number system to represent directions. Whenever a beginning point is designated, the backlink grid will indicate the direction that the path should follow; from the beginning point, all the way to the destination point. A least cost path consists of sequentially connected links that provide the route for each cell location to reach a target cell.

The least-cost path distance from a cell to a source cell is the minimum cost distance among all cost path distances from the cell to the source cells (ArcGIS 9.1, 2007).

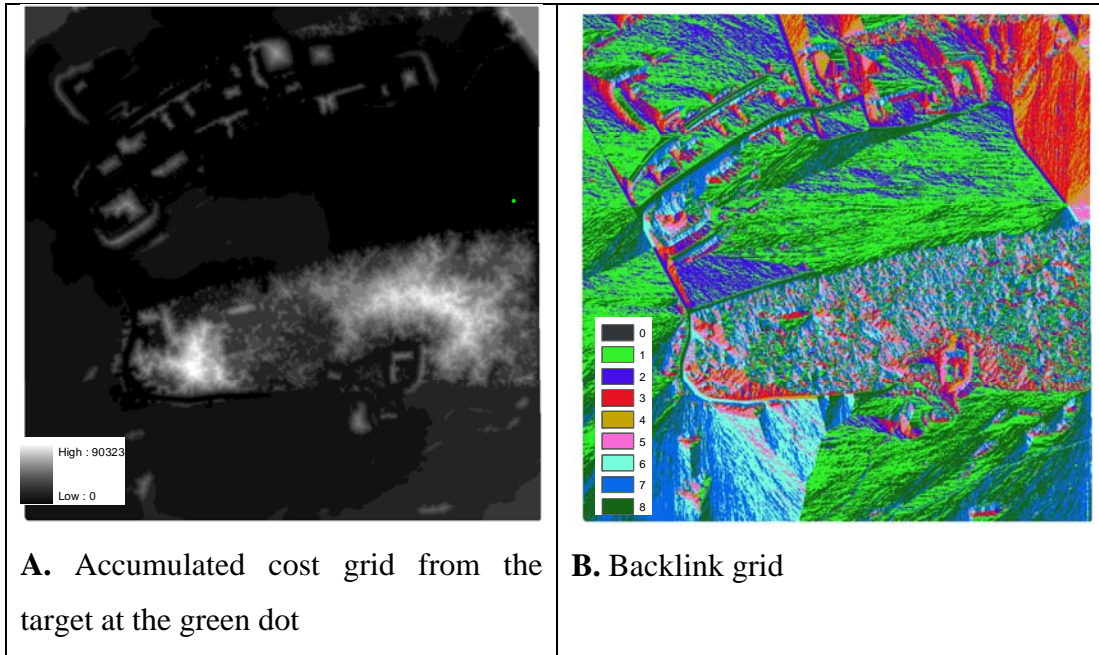


Figure 3.10: An accumulated cost grid and a Backlink grid

3.3 THE EXPERIMENT

We selected a test site for which LIDAR data was readily available. The study area makes use of Virginia Tech’s College of Agriculture & Life Sciences’ land on the western portion of campus near US 460. Figure 3.12 is a digital orthophoto of the test site taken simultaneously with the LIDAR data collection. While much of this area contains fence lines and some farm animals, the terrain and proximity to campus works well for this study. In addition, this area is currently being used by the Virginia Tech unmanned systems laboratory for tests of autonomous vehicles. Access to the imagery and LIDAR data was graciously provided by the Town of Blacksburg.

The size of the study area is large enough to illustrate navigation. The ideal size would be large enough to model variation in terrain, but small enough to validate paths. This location meets those two criteria.

Accuracy assessment of the barrier identification was done by comparing the buildings manually extracted from the ortho-photo and barriers layer of the test site. The summary of the results is shown in the table below.

Table 3.1 : Summary results of accuracy assessment

No. of pixels in ortho-photo (Buildings)	No. of pixels in barriers layer (Buildings)	No. of correctly identified pixels (Buildings)
31205	32275	29252

The result shows that 93.74 percent of the buildings pixels were correctly identified. Most of the problem areas were the margins of the buildings. The margins of buildings are generally smooth but they appear more zagged in the barriers layer (Figure 3.11).

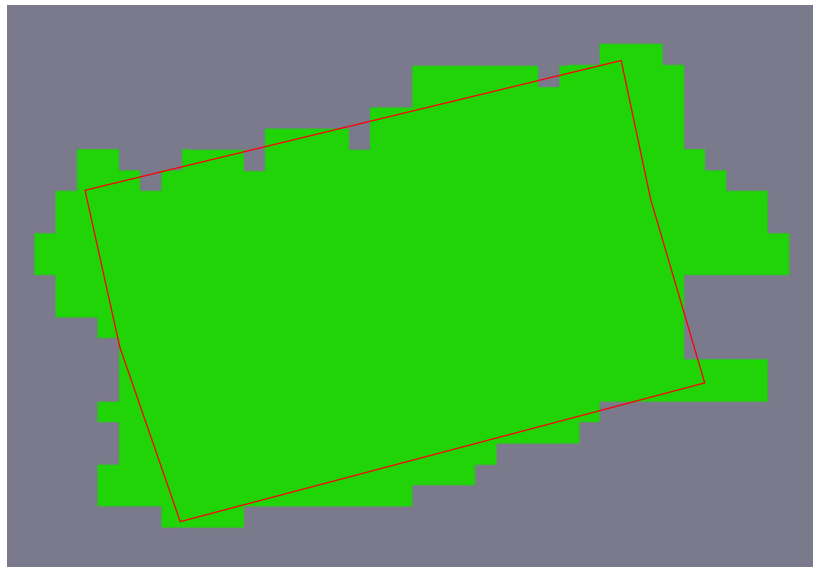


Figure 3.11: Digitized building margin overlaid on top of building extracted (Red line manually digitized building boundary from the ortho-photo, Green – Building Extracted)

In order to compare quantitatively the result of the least cost paths, ten random points were selected in the study area and 45 least cost paths and Euclidean paths were located between pairs

of those points. The Euclidean paths were used as shortest physical distance bench marks to quantify the cost, mean slope and sinuosity of the least cost paths. Figure 3.13 shows all the 45 least cost paths and their corresponding Euclidean paths. A quick visual check of the processes described above indicated that the model worked as predicted. The computed paths did not intersect any trees or buildings and, in fact, skirted around several barriers. Since the roads were assigned the least cost, most of the least cost paths followed the roads whenever practical.

The paths were then classified into two groups; paths which had no barriers and steep slopes along their Euclidean paths and paths which had barriers and steep slopes along their Euclidean paths, to see how the model functioned in each of the categories (Table 3.2).

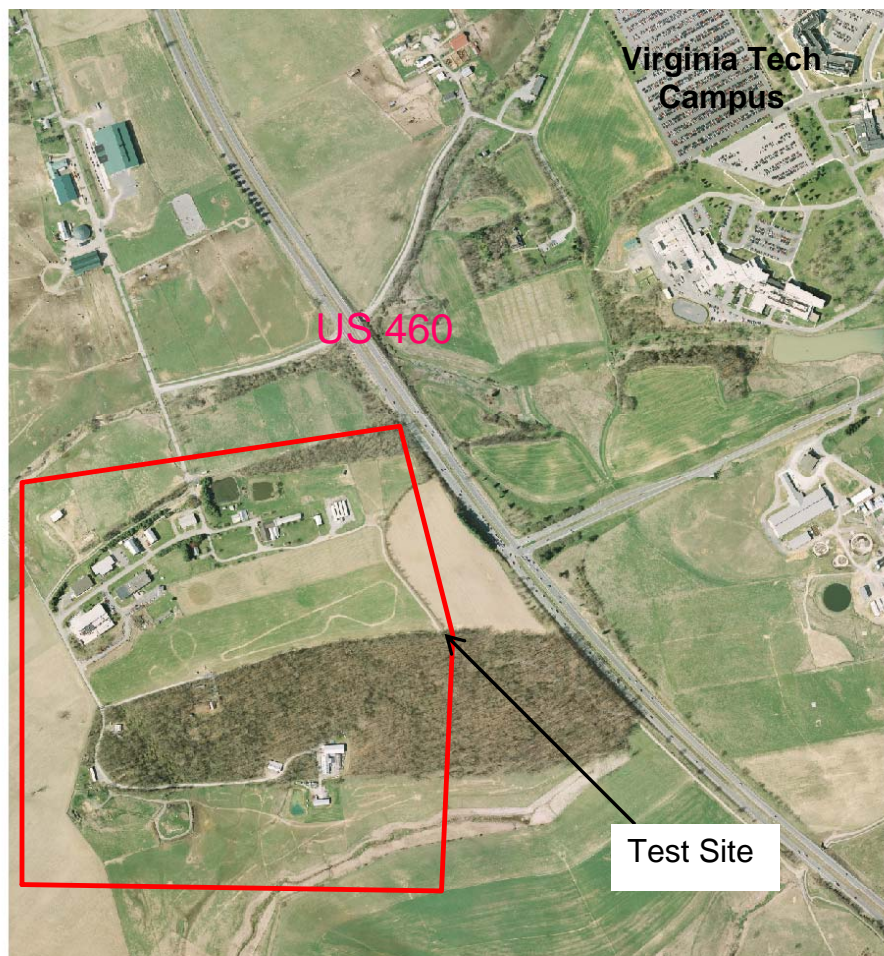


Figure 3.12: Digital orthophoto of the study area (Image reproduced with permission ©blacksburg.gov)

Table 3.2: Summary results of each category of paths in terms of average cost, average slope and average length (no. of cells).

Path Type	Least cost Paths			Euclidean paths		
	<i>Cost</i>	<i>Slope</i>	<i>Length(ft)</i>	<i>Cost</i>	<i>Slope</i>	<i>Length(ft)</i>
No barriers	3394	5.47	770	2496	7.47	540
With barriers	4086	9.73	3002	124927	23.93	1322

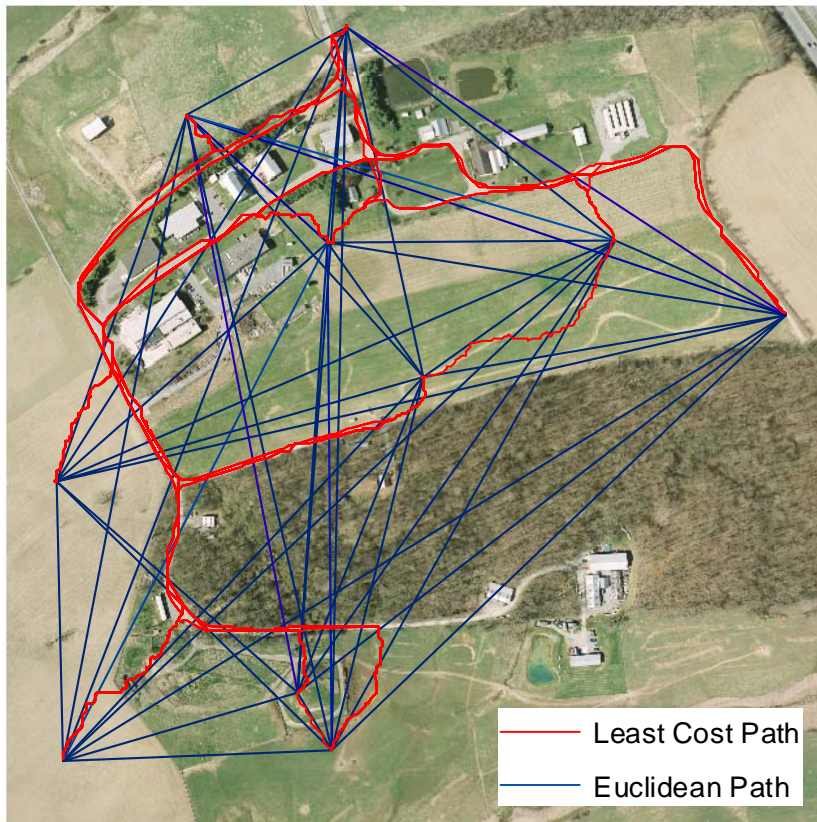


Figure 3.13: Least cost paths and the Euclidean paths (Image reproduced with permission ©Blacksburg.gov)

The accumulated surface costs of most of the least cost paths were far below those of their corresponding Euclidean paths. For individual cases in the sample of 45 paths, the histogram below shows the differential between the least cost paths minus the cost of the corresponding Euclidean path (Figure 3.14). All of the values are negative meaning that the least cost paths are more efficient. Table 3.3 shows the cost difference in both categories of paths. It is apparent that in the paths with endpoints close together (less than 950 ft) and no barriers in between, the least cost path almost follows the shortest path and the cost difference is small. In a few such cases the cost to traverse the Euclidean paths is only slightly higher than the cost of the least cost paths. But if the distance between the points is large with lot of barriers and steep slopes in between, the cost improvement of the model is great.

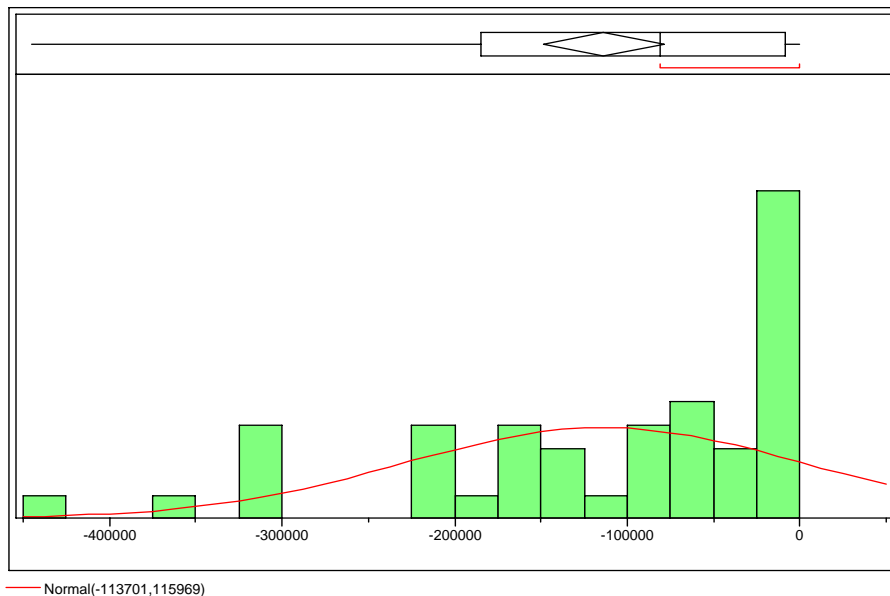


Figure 3.14: Distribution of the values of costs of least cost paths minus costs of Euclidean paths

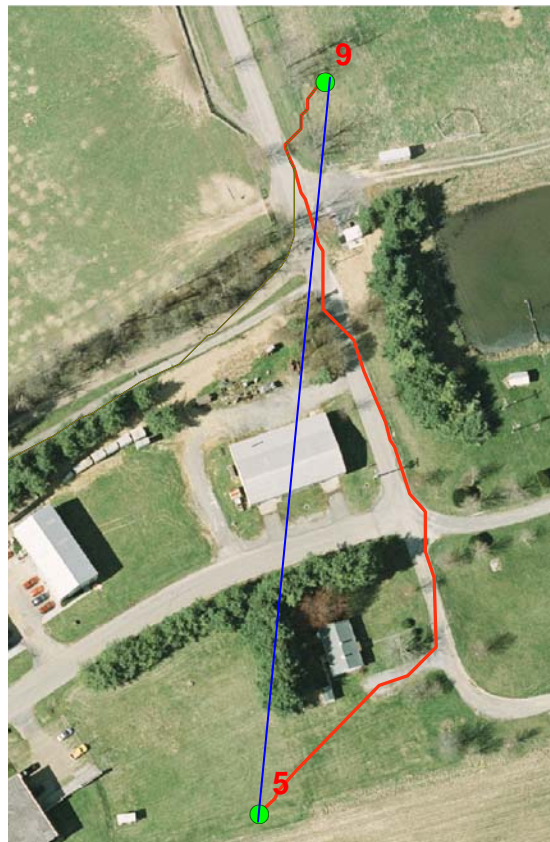
Table 3.3: Table showing the cost differential in different path types

Type of path	Mean Cost differential
Paths with close end points and no barriers in between	- 1107
Paths with far end points and barriers in between	- 129847

An example of a least cost path in which the difference between the cost of the least cost path and cost of Euclidean path is low is between the points 5 and 7 (Figure 3.15 A). In this case the distance between the points is small and there are no barriers and steep slopes between the points. In most cases like the path between points 5 and 9 (Figure 3.15 B), the least cost paths are cheaper than the corresponding Euclidean paths. The t-test done to evaluate the significance of these least-cost paths with corresponding Euclidean paths shows that the cost of traveling the least-cost paths is statistically lower at the 0.001 confidence level (Table 3.4).



A



B

Figure 3.15 A: Least cost path (Red) and Euclidean path (Blue) joining the points 5 and 7

B: Least cost path (Red) and Euclidean paths (Blue) joining the points 5 and 9.

Table 3.4: Results of t-test

If Variances Are	t statistic	Df	Pr > t
Equal	6.612	88	<0.001
Not Equal	6.612	44.01	<0.001

The average slope of the least cost path is always less than the average slope of the Euclidean paths. As the slopes above fifteen percent were assigned as barriers, the least cost paths never include slopes above that threshold. In contrast the average slopes in most of the Euclidean paths are above fifteen percent (Figure 3.16). As was true for cost, when the paths are short and have no barriers in between their endpoints, the difference between the mean slopes of the least cost paths and mean slope of Euclidean paths is not that large.

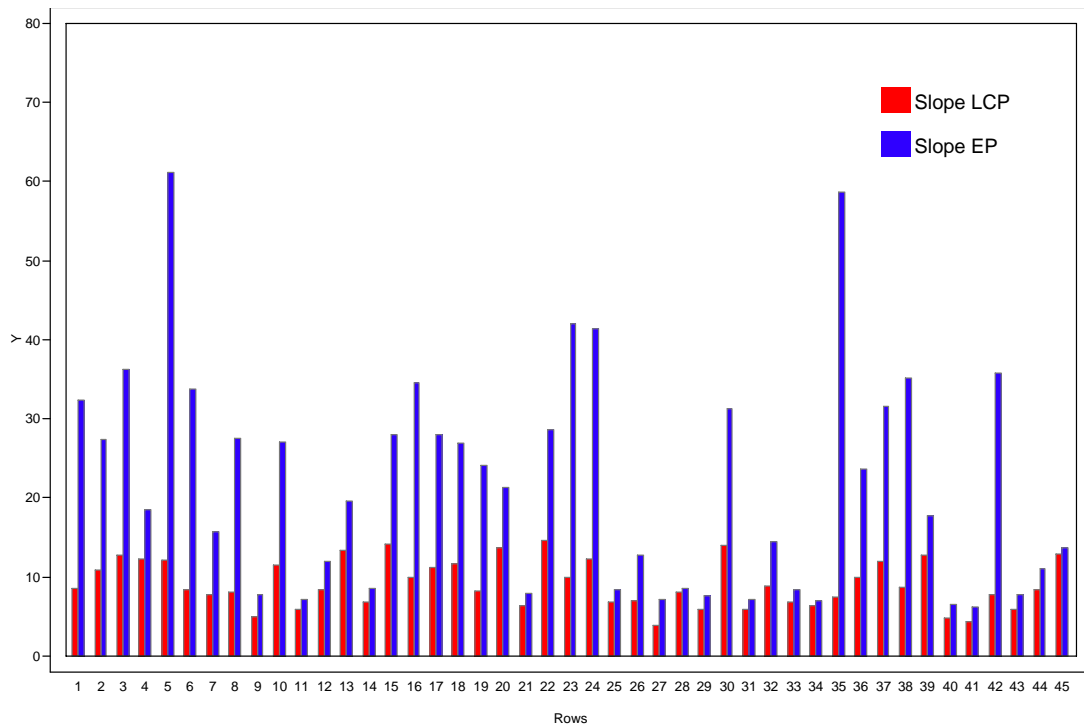


Figure 3.16: Comparison between the average slope of least cost paths and average slope of Euclidean paths

All of the least cost paths are physically longer than their corresponding Euclidean paths (Figure 3.17). The sinuosity (Table 3.5) in most of the cases depends on the area of barriers and

the steepness of the slopes in between the source and target. As with cost and slope, if the barriers along a Euclidean path are few and slope is gentle, the sinuosity is less and the least cost path almost follows the Euclidean path, but in the presence of barriers and high slopes then the sinuosity is high.

Table 3.5: Mean sinuosity of the least cost paths

Path type	Sinuosity
No Barrier	1.42
With Barriers	2.27

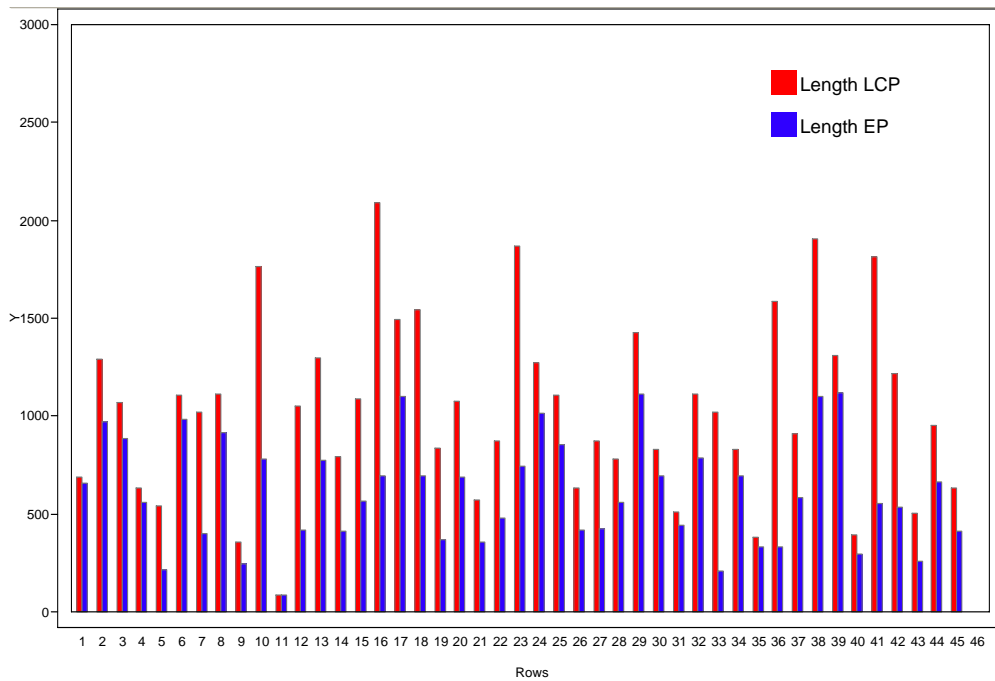


Figure 3.17: Comparison between the length of the least cost paths versus the length of the Euclidean paths.

3.4 CONCLUSION

Route selection is one of the most important and useful problems solved through application of geographic information systems. While both object extraction and least cost path finding procedures are readily available in GIS, this paper is one of the first efforts in integrating them for the purpose of autonomous ground vehicle navigation.

Most of the extracted least cost paths behave as predicted; they skirt around barriers and stay on more level slopes, following roads when it is directionally appropriate. The statistical analysis of cost, slope and length of the least-cost paths as compared to corresponding Euclidian paths shows that they are significant improvements over a “shortest distance between two points is a straight line” assumption that could be made in basic waypoint navigation. The model is at its best when distance between path endpoints is large and there are lot of barriers and steep slopes in between. A straight line assumption is efficient when the endpoints are near one another with few or no barriers in between. This discrepancy might be minimized by making slight changes in weights assigned to slope factors while creating a friction surface. For example, a vehicle might not note any difference in trafficability on a 2 degree slope as opposed to a 1 degree slope, but the current model would assign a larger cost to a cell with a 2 degree slope. A simple reclassification of costs on an equally trafficable slope set would likely align the least cost path with the Euclidean path.

In this experiment, the least cost paths were almost always superior to the base line alternatives. They did dodge obstacles appropriately, and were fully navigable routes. Further research is still in order however as there were a few exceptions to the rule. This model contains several variables which can change according to the vehicle type and functionalities. Hence, if we know the details about the vehicle like the turn radius, height clearance etc. the model can be changed in order to obtain better results for that specific vehicle. In addition there are other barriers which can affect the performance of the vehicles like plowed fields, small pits or trenches, which may not be clearly identified using LIDAR data alone. These layers, if available, need to be added up to obtain better performance of the model. LIDAR data is a big step in the correct direction, but routing algorithms cannot assure absolutely optimal results beyond the data

with which they are presented. Until real-time GIS data is implemented with all the factors necessary for navigation, it may be impossible to assure finding the optimal path, but we should always be able to find a good path.

References:

ArcGIS 9.2 desktop help, 2007, Environmental Systems Research Institute (ESRI)

Edwards, D. L., Desmond, G. B. and Schoppmann, M.W. 1988, "Terrain Database Generation for Autonomous Land Vehicle Navigation," *Photogrammetria* 43: 101-107.

Feldman, S. C., Pelletier, R. E., Walser, E., Smoot, J. C. and Ahl, D. 1996, "GIS, remote sensing analysis used to select potential route," *Pipe Line and Gas Industry*, May 1996, 52 – 55.

Jaga, R., Novaline, M., Sundaram, A., and Natarajan, T. 1993, "Wasteland development using geographic information system techniques," *International Journal of Remote Sensing*, 14, 3249 – 3257.

Lee, J. and Stucky, D. 1998, "On applying viewshed analysis for determining least-cost paths on Digital Elevation Models," *International Journal of Geographical Information Science*, Vol. 12, No. 8, 891- 905

Morgan, K and Habib, A., 2002, "Interpolation of LIDAR data and automatic building extraction," *Proceeding of ACSM – ASPRS 2002 Annual Conference*, Washington D.C. (CD – ROM)

Sithole, G., 2001, "Filtering of laser altimetry data using a slope adaptive filter," *IAPRS*, 34, 3W4

Sithole, G. and Vosselman, G., 2004, "Experimental comparison of filter algorithms for bare-Earth extraction from airborne laser scanning point clouds," *ISPRS Journal of Photogrammetry and Remote Sensing* 59, 85-101

Stahl, C. 2005, "Accumulated Surfaces & Least-Cost Paths: GIS Modeling for Autonomous Ground Vehicle (AGV) Navigation," Thesis submitted to the Department of Geography, Virginia Tech

Vosselman, G. 2000, "Slope based filtering of laser altimetry data, IAPRS, 33, Amsterdam.

Warntz, W. 1961, "Transatlantic flights and pressure patterns", The Geographical Review, Vol. 51, 187-212, 1961

Weidner, U and Forstner, W. 1995, "Towards automatic building extraction from high resolution digital elevation models," ISPRS Journal of Photogrammetry and Remote Sensing, Vol.50 pp 38 – 49

Zhang, K., Chen, S., Whitman, D., Shyu, M., Yan, J. and Zhang, C. 2003, "A progressive morphological filter for removing nonground measurements from airborne LIDAR data," IEEE Transactions on geoscience and remote sensing, Vol. 41, No. 4 pp 872-882

Vita

Om Poudel was born in the small, mountainous country of Nepal on October 2, 1977. He attended Tribhuvan University, Kathmandu, Nepal where he earned Bachelor and Master in science degrees in Geology. In the fall 2005, he enrolled in the Graduate school at Virginia Tech to pursue his education in Geographic Information Systems and Remote Sensing. He is currently working as a Geospatial technician at USDA, NRCS East Remote Sensing Lab, Greensboro, NC.